PHYSOR 2014 - The Role of Reactor Physics toward a Sustainable Future
The Westin Miyako, Kyoto, Japan, September 28 - October 3, 2014, on CD-ROM (2014)

VALIDATION OF CASMO5 SPENT FUEL ISOTOPICS WITH DECAY AND FISSION YIELD UNCERTAINTIES

Joshua Hykes and Joel Rhodes*
Studsvik Scandpower, Inc.
1070 Riverwalk Drive, Suite 150
Idaho Falls ID 83402, USA
joshua.hykes@studsvik.com
joel.rhodes@studsvik.com

ABSTRACT

We examine the effects of the uncertainty in decay and fission yield data on CASMO5-computed nuclear fuel isotopics, comparing the results to measurements. The uncertainties of radioactive decay constants, decay and (n,γ) capture branching fractions, and fission yields are extracted from the ENDF/B-VII.1 data files or estimated where they are lacking. These nuclear data uncertainties are propagated through the CASMO5 lattice depletions via Monte Carlo sampling. The distribution of computed isotopic compositions are compared to the Fukushima Daini-2 measurements of Nakahara. The uncertainties in the calculated values are able to explain some of the calculation-to-measurement discrepancies, particularly for ^{242m}Am and the samarium isotopes.

Key Words: **isotopic validation, propagation of uncertainty**

1. INTRODUCTION

Monte Carlo sampling using randomly perturbed input data is a simple method for the propagation of uncertainty through a model. This technique has been applied to burnup calculations by several researchers [1–6]. Williams et al. have demonstrated the usefulness of Monte Carlo sampling methods for the propagation of uncertainty in lattice depletion calculations [5, 6]. In the sampling method, the input parameters of interest are independently and randomly perturbed according to their estimated uncertainty. A set of lattice calculations are then performed with the perturbed input data. Finally, statistics are generated from the distribution of responses computed by the lattice calculation.

In this paper, a similar technique is applied to examine the effects of decay and fission yield uncertainties on the comparison of CASMO5-calculation versus measurements of spent fuel inventory from a BWR lattice burned at Fukushima Daini-2 published by Nakahara [7]. The methods are applied with the new "202" CASMO5 nuclear data library. The 202 data library

*studsvik.com/nfa

- is based on ENDF/B-VII.1 [8] but supplemented by TENDL-2012 [9],
- uses 586 energy groups (same as predecessor "201" library),
- contains 1095 nuclides or materials with full or absorption-only cross section models (526 more than predecessor 201 library),
- models 119 heavy nuclides and 491 fission products in the depletion calculation (the 201 library used 60 and 259, respectively),
- and was processed with NJOY2012.8 (the 201 library used NJOY99.364).

The source of the nuclear data uncertainties is discussed in section 2. The results of the propagation of uncertainty through the BWR lattice calculation are given in section 3.

2. NUCLEAR DATA UNCERTAINTIES

In the preparation of the CASMO5 202 library, uncertainties for the decay data and fission yields were extracted along with the mean or nominal values. There were four types of nuclear data uncertainties considered: decay constants, decay branching fractions, (n,γ) capture branching fractions to metastable states, and fission yields. The source of each data uncertainty is outlined in this section, as well as the methods used to randomly perturb the data for input to the set of depletion calculations.

2.1. Radioactive Decay Constants

Decay constants are needed to compute the decay of radioactive nuclides during the depletion calculation. The half-lives and their associated 1σ uncertainties are given in File 8, MT=457 of the ENDF library. The uncertainties are typically quite small; for most important nuclides the relative standard deviation is less than 1%. Since the decay constants are each independent, sampling can be done one-by-one, drawing randomly from a normal distribution centered at the nominal value.

2.2. Decay Branching Fractions

Some nuclides have multiple decay pathways, where they may decay via two or more modes out of beta, electron capture, isomeric transition, alpha decay, neutron emission, or spontaneous fissions. The branching fractions specify how much of each daughter nuclide is produced. The branching fraction nominal value and 1σ uncertainty are given in ENDF File 8, MT=457. As Williams notes [5], sampling random values for a parent nuclide's branching fractions should be done in concert so that the fractions sum to one. For a nuclide with n decay pathways, the first $n-1$ decay fractions f_i are sampled independently. Then the last decay fraction is computed as $f_n = 1 - \sum_i^{n-1} f_i$.

2.3. Capture Branching Fractions

Another important branching fraction is that of (n,γ) capture to a ground or metastable state. Although this branching fraction is dependent on the incident neutron energy, CASMO5 approximates the fraction as a constant, using a value from the thermal energy range. An important example of this reaction is $^{241}\mathrm{Am} + {}^{1}_{0}\mathrm{n} \rightarrow {}^{242\mathrm{m}}\mathrm{Am}$. Unlike the other types of data considered here, the uncertainties for capture branching fractions do not appear directly in the ENDF files. Instead, we estimate the capture branching fraction uncertainties with the following two steps, preferring the first but falling back to the second when necessary.

1. Use the thermal capture cross sections from Mughabghab's Atlas of Neutron Resonances [10]. For many of the reactions of interest, the thermal capture cross sections to ground and to metastable state are given with uncertainties. Linear propagation of error is used to estimate the resulting uncertainty in the capture branching fraction. This relative uncertainty is then applied to the branching fraction in CASMO5. For example, suppose the thermal capture cross section to the ground state is $\sigma_\gamma^g = g \pm \sigma_g$ and to the metastable state is $\sigma_\gamma^m = m \pm \sigma_m$. Then the branching fraction to the metastable state is given by

$$f_m = \frac{\sigma_\gamma^m}{\sigma_\gamma^g + \sigma_\gamma^m} = \frac{m}{g+m} \quad , \tag{1}$$

   and the relative variance is

$$\left(\frac{\sigma_{f_m}}{f_m}\right)^2 = \frac{g^2\sigma_m^2 + m^2\sigma_g^2}{m^2\,(g+m)^2} \quad , \tag{2}$$

   where we used a first-order Taylor series expansion for the error. The correlation between the measured values of σ_γ^g and σ_γ^m is assumed zero for lack of better information. The relative standard deviation from Equation 2 is taken as the uncertainty for the value in CASMO5.
2. If data is unavailable in the Atlas of Neutron Resonances, then the standard deviation is assumed to be one third of the smallest branching fraction f_s. A 3σ interval would then bracket the perturbed fraction $\tilde{f}_s \in [0, 2f_s]$, which is hoped to be sufficiently conservative.

The sampling perturbations for capture branching fractions are performed in a similar manner as for the decay branching fractions.

2.4. Fission Yields

Fission yields and associated 1σ uncertainties are available on ENDF File 8, MT=454 for independent yields (IY) and MT=459 cumulative yields (CY). The CASMO5 202 nuclear data library contains fission yields for a particular incident neutron energy for each fissioning nuclide. Otherwise, the yields are assumed to be independent of energy. The library uses a combination of independent and cumulative yields. Cumulative (or partial cumulative) yields are used for those CASMO5 fission products which have radioactive decay precursors which are not modelled in CASMO5. Those cumulative or partial-cumulative yields are computed from the summation of the precursor independent yields, making sure to account for branching fractions. The uncertainties for these

CYs are computed with linear propagation of error through the sum of independent yields. As Williams observes [6], the fission yields along a decay chain are correlated, and he handles these correlations by assigning non-zero off-diagonal elements in the yields covariance method. The method is attributed to M. Pigni, but it is not described in detail.

Lacking the details for the approach from Reference [6], we instead adjust the relative standard deviation of the CY so that it matches the CY of the end-of-chain nuclide. The purpose is to avoid introducing larger-than-realistic uncertainties into fission products at the end of decay chains. For example, ^{120}Cd is on the southeast boundary of the fission products modelled, so it uses a CY. Since the uncertainties in its precursor IYs are large, the CY has a large uncertainty (roughly 50% relative standard deviation for a fission of ^{235}U). However, ^{120}Cd decays rapidly through ^{120}In to ^{120}Sn, which is stable. The ENDF/B-VII.1 uncertainty for the ^{235}U to ^{120}Sn CY is 8%. If the high CY uncertainty for ^{120}Cd were introduced into the perturbed system, its large effect would quickly be felt by ^{120}Sn. Our approach to this difficulty is to reduce the relative uncertainty of ^{120}Cd to match the relative uncertainty of the CY for ^{120}Sn. While this underestimates the uncertainty of the yields to ^{120}Cd, we judge it more important to match the uncertainty of the stable end-of-chain ^{120}Sn. A similar procedure is followed for all nuclides using CYs along the southeast border of the fission product block. Figure 1 illustrates the effect of these adjustments to the standard deviation. The fission yields are summed over isobaric (same mass number A) nuclides for a simpler figure. Figure 1a shows the yields as they were from computed from the ENDF/B-VII.1 IYs. Notice the large uncertainties. Figure 1b shows the same plot for the fission yields whose CY relative uncertainties had been adjusted to match the end-of-chain stable nuclide.

Our approach for perturbing the fission yields is similar to that of Williams, with the difference that he includes non-zero covariance terms. First the yields are independently and randomly perturbed according to their assumed normal distribution. Then the yields are normalized such that their sum equals 2.0.

3. UNCERTAINTY PROPAGATION VIA MONTE CARLO

3.1. Monte Carlo Sampling Procedure

Propagating uncertain inputs using Monte Carlo sampling is a widely known technique, and software libraries are available to automate such a task [11]. In this work, a script external to CASMO5 perturbed the nuclear data inputs, executed the CASMO5 case with the perturbed inputs, and then collected the calculated responses. Special input options to CASMO5 were introduced which allowed for the perturbation of the decay and fission yield data.

3.2. Comparisons with Fukushima Daini-2 Measurements

To validate the CASMO5 calculation, the isotopic compositions measured in the BWR case from Reference [7] are compared to the computed values from CASMO5. These measurements are for

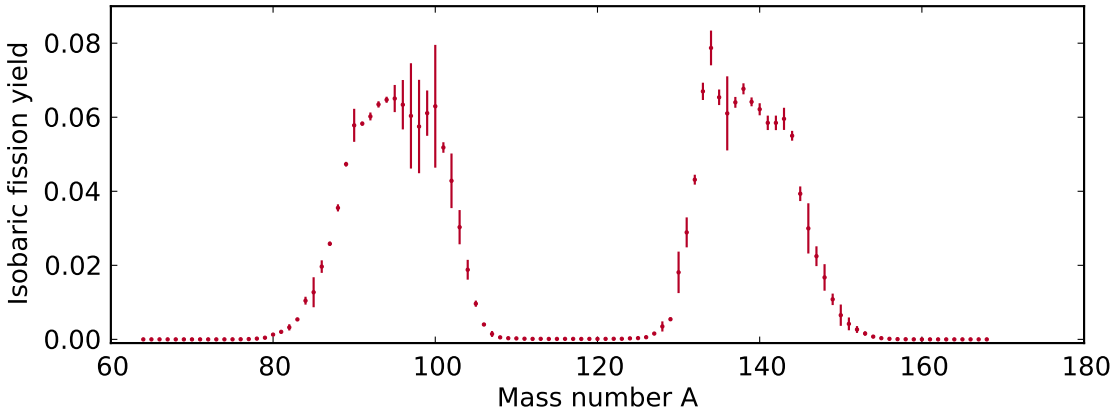

(a) Default ENDF/B-VII.1 independent yield uncertainties.

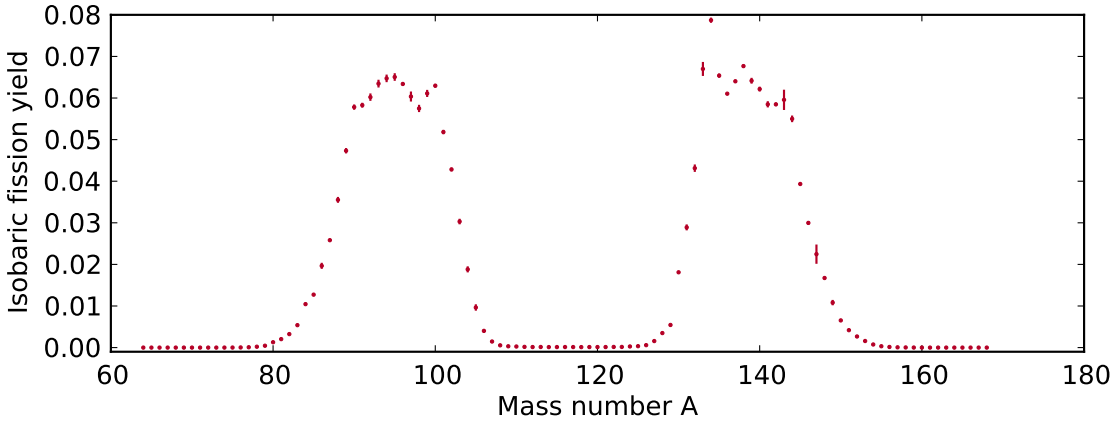

(b) Uncertainties adjusted to match end-of-chain nuclide.

Figure 1: Fission yields for ^{235}U summed over isobaric nuclides. Data is from ENDF/B-VII.1. Errorbars are 1σ uncertainties.

Table I: Burnups for the sample locations in pins SF98 and SF99.

Sample ID	Burnup (MWd/kgU)	Sample ID	Burnup (MWd/kgU)
SF98-1	4.2	SF99-1	7.5
SF98-2	26.5	SF99-2	22.6
SF98-3	36.9	SF99-3	32.4
SF98-4	42.4	SF99-4	35.4
SF98-5	44.0	SF99-5	37.4
SF98-6	39.9	SF99-6	32.4
SF98-7	39.4	SF99-7	32.1
SF98-8	27.2	SF99-8	21.8
		SF99-9	16.7
		SF99-10	7.2

two fuel pins burned in the Fukushima Daini-2 BWR from 1989 to 1991. The fuel pins in the report are named SF98 and SF99. Eight axial locations are measured for pin SF98 and ten for SF99. The initial composition of the fuel pins vary axially. There are axial locations with natural uranium, enriched uranium, and enriched uranium with gadolinium poison. The sample burnups are given in Table I. SF98 was cooled for 5.5 years before measurement, while SF99 was cooled for 6.5 years. The operating history of the fuel assembly is given in the reference.

Studsvik has existing CASMO5 models of these lattices. For this work, these models were adapted to allow for the perturbation of nuclear data.

The Monte Carlo sampling was performed with 150 samples. Each sample involved 18 CASMO5 lattice depletions, one for each axial measurement location. (Since the SF98-2 location was ignored, only 17 depletions were necessary.) The number of samples was increased until the standard deviations converged. From these samples, the mean and standard deviation were computed for the isotopic compositions. Then the computed results C were compared with the measurements E with the $C/E - 1$ metric. Figure 2 shows this comparison for all of the measurement locations except SF98-2, the results for which are discounted by Nakahara as likely having an error in the measurements. Nakahara also notes that the measurements for ^{106}Ru and ^{125}Sb are underestimates of the true value because of their lack of solubility in the processing of the spent fuel. Indeed, the CASMO5 estimates of these values are higher than the measurements in all but two cases.

In Figure 2, the results are sorted according to segment type. The measurement-to-calculation discrepancies for the SF98-1 and SF99-1 locations are noticeably larger than at the other locations for a number of nuclides. The short distance of these segments from axial fuel changes (39 mm for SF98-1 and 21 mm for SF99-1) may be causing a breakdown in the 2D lattice modelling assumption used in CASMO5. However, this degradation in accuracy is not observed for SF99-9 or SF99-10, which are only 15 mm and 34 mm, respectively, from axial changes.

The numerical values for location SF99-5 pictured in the bottom subplot of Figure 2 are provided in Table II for actinoids and Table III for fission products.

Ideally the computed value or its 95% error bar would overlap with measurement error represented by the gray shaded region. For the samarium isotopes, ^{154}Eu, and ^{242m}Am, the computed uncertainty provides an overlap with the measurement where an overlap had not already existed. However, unexplained discrepancies still exist for the cesium isotopes and for many of the actinoids. The decay and fission yield uncertainties have minimal effects on the actinoids. The uncertainty for ^{242m}Am comes from the capture branching fraction.

Williams has included the effects of cross section, decay, and fission yield uncertainties for a sample PWR lattice [6]. If their reported uncertainties are representative of the size of errors for the presently considered BWR lattices, then some of the discrepancies for the actinoids would be explainable. For instance, Williams reports the 1σ uncertainty for ^{238}Pu is about 4% in the 10–40 MWd/kgU range pertinent for the Nakahara measurements. Thus, the 2σ/95% interval would explain the observed discrepancy for most of the measurement locations for ^{238}Pu.

Even with the uncertainties reported in Reference [6], the discrepancies are still larger than expected for ^{241}Am and the curium isotopes, especially ^{242}Cm. There are several ^{241}Am measurements with $C/E - 1$ greater than or approximately equal to 20%, while Williams reports a 1σ uncertainty of less than 3%. Likewise for ^{242}Cm, most of the CASMO5 estimates are 20–60% lower than the measurement, while the 1σ uncertainty from Williams is less than 4%. Since ^{242}Cm is a strong α emitter in spent fuel, accurately predicting its concentration is important.

4. CONCLUSION

We have compared CASMO5 calculations using the new 202 nuclear data library against the BWR spent fuel measurements published by Nakahara from a fuel assembly burned in Fukushima Daini-2. The uncertainties for decay constants, decay and capture branching fractions, and fission yields were propagated through the CASMO5 calculation using Monte Carlo sampling. For most of the nuclides and fuel sample locations, the difference between CASMO5 and the experiment is less than 20%. The propagated uncertainties explain observed calculation-to-measurement discrepancies for several samarium isotopes, ^{154}Eu, and ^{242m}Am. The differences for these nuclides were larger than the reported measurement error, but the propagated nuclear data uncertainties were larger or similar in magnitude to the observed differences. However, significant differences still exist for the higher actinoids, especially ^{241}Am and ^{242}Cm, which have larger errors than either the measurement or propagated nuclear data uncertainty.

Table II: Actinoid comparison for location SF99-5 of the measurement-to-calculation discrepancy, the CASMO5-estimated uncertainty, and uncertainties from Williams. Although the uncertainties from Williams and Martínez are for PWR lattices, they are copied here for reference. For the actinoids (with the exception of ^{242m}Am), it is clear from the CASMO5 column that the decay and fission yield uncertainties have little effect.

		1σ uncertainty (%)		
Nuclide	$C/E - 1$ (%)	CASMO5[a]	Williams [5, 6][b]	Martínez [2][c]
^{234}U	12.4	0.1	4	4
^{235}U	5.5	0.1	1	1
^{236}U	−1.0	0.0	2	1
^{238}U	0.0	0.0	0	0.2
^{237}Np	−12.5	0.1	5	2
^{238}Pu	29.6	0.3	6	2
^{239}Pu	0.2	0.1	1.5	4
^{240}Pu	−5.5	0.0	2	8
^{241}Pu	7.2	0.1	2	5
^{242}Pu	2.7	0.0	3	3
^{241}Am	−16.3	0.1	3	4
^{242m}Am	−1.0	8.5		
^{243}Am	−0.6	0.1	9	6
^{242}Cm	−71.6	0.4	3	
^{243}Cm	0.3	1.3		
^{244}Cm	1.2	0.1	10	6
^{245}Cm	6.4	0.2	16	
^{246}Cm	−19.5	0.1	16	15
^{247}Cm	−30.1	0.1		

[a] The CASMO5 uncertainty includes the effect of uncertainties from decay and fission yield data.
[b] The Williams uncertainties include the cross section uncertainties as well as the decay and fission yield data. The values listed are the maximum uncertainty over the interval 10–40 MWd/kgU, which covers most of the experimental range.
[c] The Martínez uncertainties include the cross section uncertainties as well as the decay and fission yield data. The values are from Table IV.2 in [2]; the burnup in that case is 42.5 MWd/kgU.

Table III: Fission product comparison for location SF99-5 of the measurement-to-calculation discrepancy, the CASMO5-estimated uncertainty, and uncertainties from Williams. The comments of Table II apply here as well.

		1σ uncertainty (%)		
Nuclide	$C/E - 1$ (%)	CASMO5	Williams [5, 6]	Martínez [2][a]
^{106}Ru	146.1	8.8		
^{125}Sb	80.2	32.7		
^{134}Cs	−12.0	2.7	5	6
^{137}Cs	−4.7	0.8	0	3
^{144}Ce	−6.4	2.4	0.1	6
^{143}Nd	−0.2	3.8	1.5	
^{144}Nd	−2.1	1.8		
^{145}Nd	0.8	0.5	1.5	
^{146}Nd	−0.7	0.8		
^{148}Nd	0.5	3.5	0.5	
^{150}Nd	1.4	0.5		
^{147}Sm	−1.8	5.5		4
^{148}Sm	−12.2	5.3		3
^{149}Sm	10.7	4.4		16
^{150}Sm	−2.8	3.9		3
^{151}Sm	−3.6	2.0		7
^{152}Sm	−2.2	2.1		5
^{154}Sm	−2.2	12.6		3
^{154}Eu	1.1	5.2	8	23

[a] The Martínez uncertainties are the square root of the sum of squares for the cross section and fission yield errors.

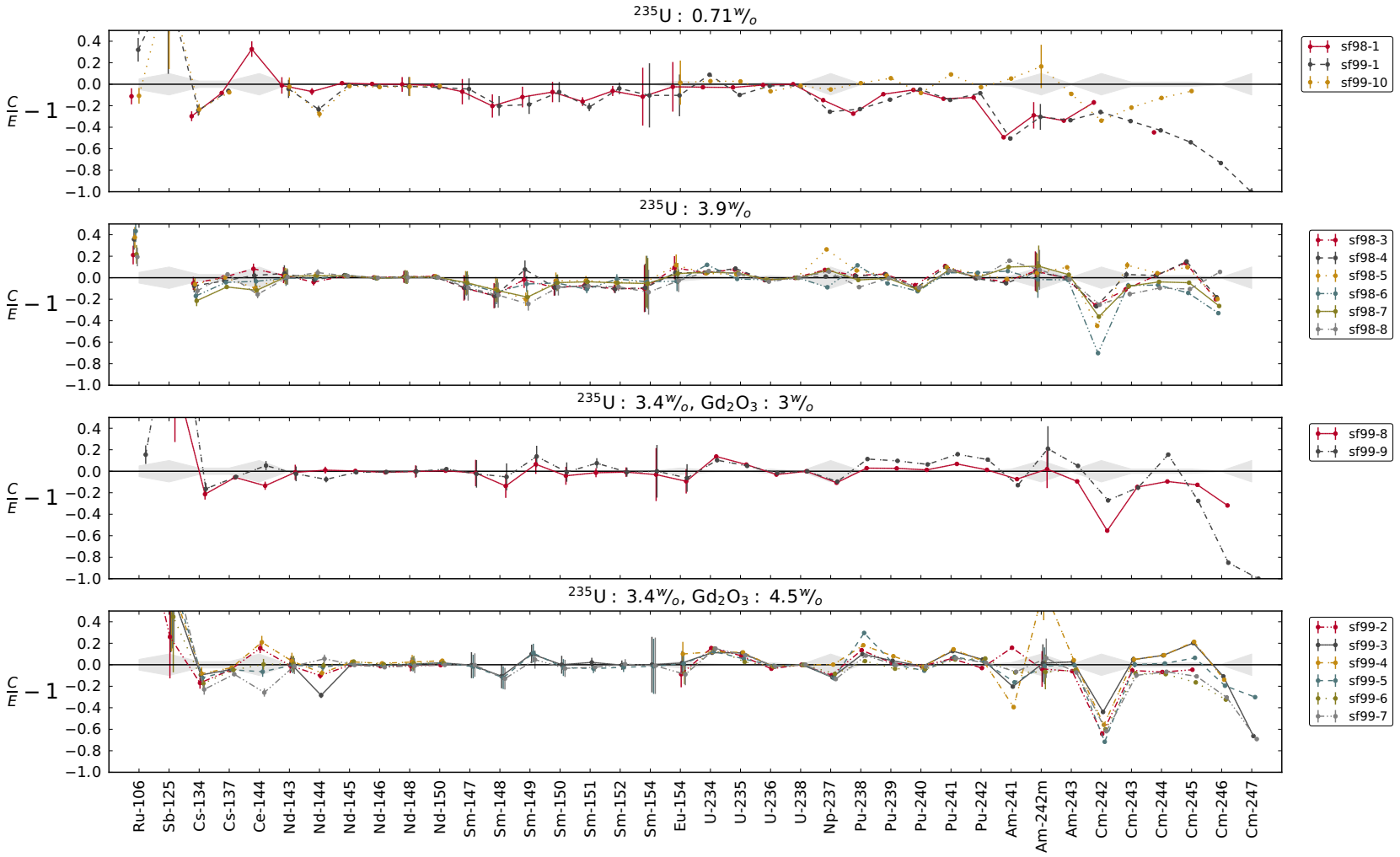

Figure 2: Comparing the computed (C) and experimental (E) values of the isotopic composition for the Fukushima Daini-2 BWR benchmark of Nakahara et al. [7]. The grey shaded region around $C/E - 1 = 0$ represents the maximum measurement error as given by Nakahara. The error bars are two standard deviation (95%) uncertainties as computed by the propagation of the nuclear data uncertainties through the CASMO5 calculation. As the horizontal axis represents discrete quantities, lines connecting points are intended only as a visual cue. The data points at each nuclide have been moved slightly left or right to visually separate the error bars.

REFERENCES

[1] N. García-Herranz *et al.* "Propagation of statistical and nuclear data uncertainties in Monte Carlo burn-up calculations." *Annals of Nuclear Energy*, **35(4)**: pp. 714–730. ISSN 0306-4549. URL http://dx.doi.org/10.1016/j.anucene.2007.07.022 (2008).

[2] J. Martínez *et al.* "Isotopic prediction calculation methodologies: application to Vandellos-II reactor cycles 7–11." In: *Proceedings of the International Conference on Mathematics and Computational Methods Applied to Nuclear Science and Engineering, M&C 2011*. Taylor & Francis. Rio de Janeiro, Brazil, May 8-12 (2011).

[3] O. L. Cabellos de Francisco *et al.* "Propagation of nuclear data uncertainties in transmutation calculations using ACAB code." *Journal of the Korean Physical Society*, **59(2)**: pp. 1268–1271 (2011).

[4] C. Dìez *et al.* "Monte Carlo uncertainty propagation approaches in ADS burn-up calculations." *Annals of Nuclear Energy*, **54**: pp. 27–35. ISSN 0306-4549. URL http://dx.doi.org/10.1016/j.anucene.2012.10.033 (2013).

[5] M. L. Williams *et al.* "A statistical sampling method for uncertainty analysis with SCALE and XSUSA." *Nuclear Technology*, **183(3)**: pp. 515–526. URL http://info.ornl.gov/sites/publications/Files/Pub37099.pdf (2013).

[6] M. Williams *et al.* "SCALE uncertainty quantification methodology for criticality safety analysis of used nuclear fuel." In: *Proceedings of ANS NCSD 2013-Criticality Safety in the Modern Era: Raising the Bar*. URL http://info.ornl.gov/sites/publications/files/Pub44063.pdf. Wilmington, NC, USA, September 29–October 3 (2013).

[7] Y. Nakahara *et al.* "Nuclide composition benchmark data set for verifying burnup codes on spent light water reactor fuels." *Nuclear technology*, **137(2)**: pp. 111–126 (2002).

[8] M. Chadwick *et al.* "ENDF/B-VII.1 nuclear data for science and technology: Cross sections, covariances, fission product yields and decay data." *Nuclear Data Sheets*, **112(12)**: pp. 2887–2996. ISSN 0090-3752. URL http://dx.doi.org/10.1016/j.nds.2011.11.002. Special Issue on ENDF/B-VII.1 Library (2011).

[9] A. Koning and D. Rochman. "Modern nuclear data evaluation with the TALYS code system." *Nuclear Data Sheets*, **113(12)**: pp. 2841–2934. ISSN 0090-3752. URL http://dx.doi.org/10.1016/j.nds.2012.11.002. Special Issue on Nuclear Reaction Data (2012).

[10] S. Mughabghab. *Atlas of Neutron Resonances: Resonance Parameters and Thermal Cross Sections. Z=1-100*. Elsevier Science. ISBN 9780080461069 (2006).

[11] B. Kleb, R. Thompson, and C. Johnston. "Blurring the inputs: A natural language approach to sensitivity analysis." In: *18th AIAA Computational Fluid Dynamics Conference*. American Institute of Aeronautics and Astronautics. URL http://dx.doi.org/10.2514/6.2007-4206 (2007).